Hindawi
Geofluids
Volume 2021, Article ID 6667245, 13 pages
https://doi.org/10.1155/2021/6667245

Research Article

A Study on the Creep Characteristics of Airport Viscous Subsoil Based on Unsaturated Stress Level

Jun Feng,[1,2] **Yue Ma**,[3] **and Zaobao Liu**[2]

[1]*School of Airport Engineering and Transportation Management, Civil Aviation Flight University of China, Guanghan 618307, China*
[2]*School of Resources and Civil Engineering, Northeastern University, ShenYang 110004, China*
[3]*School of Civil Engineering, University of Leeds, Leeds LS2 9JT, UK*

Correspondence should be addressed to Jun Feng; sckid1987@163.com

Received 24 October 2020; Revised 13 December 2020; Accepted 6 January 2021; Published 15 January 2021

Academic Editor: Chun-Hui Lu

The present study takes the ratio of the matric suction to the net vertical stress and the ratio of the matric suction to the net mean stress as new unsaturated stress levels f and F, respectively. Based on the laboratory tests and theoretical derivation, the modified one-dimensional Mesri creep model and three-dimensional creep model were established, which takes the unsaturated stress level into account. Then, the one-dimensional and three-dimensional creep characteristics of the unsaturated viscous subsoil of an airport under different unsaturated stress levels were analyzed. The following conclusions could be drawn: (1) under different stress levels, the one-dimensional creep deformation of unsaturated soil has a power function relationship with time, and the change rate exponentially decreases with the stress level, which can be well-expressed by the proposed modified one-dimensional Mesri creep model; (2) under different stress levels, the three-dimensional creep strain of the unsaturated soil shows a hyperbolic curve with time and a near-linear relationship at the semilogarithmic coordinate, which can be well-expressed by the proposed modified three-dimensional creep model; (3) under different stress levels, both the one-dimensional creep and three-dimensional creep of the unsaturated soil can be divided into two stages, which are the accelerated creep stage and stable creep stage.

1. Introduction

The "three-surface and one-body" control theory in civil aviation geotechnical design puts forward high requirements for the postconstruction settlement of the subsoil of the "basal surface," "free surface," "interface surface," and "filling body." Among these, the postconstruction settlement of an airfield runway may not exceed 20~30 cm (2013) [1]. Such requirement is likely to grow as air travel becomes more common. The postconstruction settlement of subsoil is mainly correlated to the creep characteristics of soil. The saturated soil theory is relatively mature. Hence, it is widely used in the field of engineering. However, due to moisture evaporation and engineering filling, a large amount of airport subsoil is in the unsaturated state. Thus, the unsaturated soil theory is more applicable for the study of creep characteristics of airport subsoil and is more in line with specific conditions in engineering. Furthermore, this can more accurately help with the design, construction, and operation of airport engineering.

In the unsaturated soil theory, the influence of the matric suction inside the soil on various engineering properties should be taken into account, which is the biggest difference between the unsaturated soil theory and saturated soil theory. Present studies tend to control for a single factor. Garcia et al. carried out numerically analysis to the generation of pore water pressure and deformations for unsaturated soil [2]. Han and Vanapalli carried out the nonlinear stiffness-suction and shear strength-suction relationships for unsaturated soils within the lower suction range from the nonlinearity of the soil-water characteristic curve [3]. Dorival et al. developed a solution of liquid-gas-solid coupled equations with considering the dynamics and hysteretic retention behavior for unsaturated soil [4]. Li et al. analyzed the

secondary consolidation characteristics of unsaturated soil based on the control of gas pressure [5]. Wu et al. developed an analytical solution to solve 1D deformation and rain water infiltration for unsaturated soil with controlling the matric suction [6]. By controlling the matric suction, Xiao et al. carried out a study on the deformation characteristics of unsaturated silty clay on the side slope of the reservoir bank in a hydropower project based on the consolidated drained triaxial compression test [7]. By means of laboratory tests on matric suction control, Sun et al. analyzed the triaxial creep deformation characteristics of typical northern red clay in Lantian, Shaanxi province, China [8].

It can be observed from the microstructure and mechanical mechanism of soil that matric suction is a kind of structural resistance of unsaturated soil and that the increase in matric suction has a certain "hardening" effect on soil. That is, this increases the resistance to deformation of soil. Therefore, matric suction can be regarded as a kind of "resistance" inside the soil, while other additional loads on the soil, such as vertical stress and mean stress, can be regarded as "external forces." Obviously, different forms of macroengineering characteristics of soil, such as strength and deformation, can only arise from the joint work of "internal" and "external" forces, while during the performance of various forms of engineering characteristics of soil, these "internal" and "external" forces also experience a dynamic adjustment process of coordination and common change. When a test or related simulation is conducted, a stress form that can simultaneously reflect the "internal" and "external" forces should be defined [9–16]. Thus, the present study defined a new stress level for unsaturated soil and introduced such stress level into the tests and model research, in order to study the creep characteristics of unsaturated soil in practical engineering.

2. Unsaturated Stress Level

2.1. One-Dimensional Stress Level. In the one-dimensional creep deformation of unsaturated soil, the soil was subjected to the combined effect of internal matric suction and external net vertical stress. The ratio of the matric suction to the net vertical stress was taken as the one-dimensional unsaturated stress level f, and f can be expressed as:

$$f = \frac{u_a - u_w}{\sigma_1 - u_a} = \frac{s}{\sigma_1 - u_a}. \tag{1}$$

In the formula, f is the ratio of the matric suction to the net vertical stress, u_a is the pore gas pressure, u_w is the pore water pressure, σ_1 is the net vertical stress, and s is the matric suction.

2.2. Three-Dimensional Stress Level. In the three-dimensional creep deformation of unsaturated soil, the soil was subjected to stresses from three directions. The net mean stress was used to represent the net external force after pore air pressure was deducted. The ratio of the matric suction to the net mean stress was taken as the three-dimensional unsaturated stress level F, and F can be expressed as:

$$F = \frac{u_a - u_w}{\bar{\sigma} - u_a} = \frac{s}{\bar{\sigma} - u_a}. \tag{2}$$

In the formula, $\bar{\sigma}$ is the net mean stress, and its expression is:

$$\bar{\sigma} = \frac{\sigma_1 + \sigma_2 + \sigma_3}{3}. \tag{3}$$

In the expression, σ_1, σ_2, and σ_3 are the stresses from three directions to which the unsaturated soil is subjected, and F is the ratio of the matric suction to the net mean stress.

3. One-Dimensional Creep Characteristics

3.1. Modified One-Dimensional Mesri Creep Model. In 1968, Singh-Mitchell proposed using the exponential function to describe the one-dimensional stress-creep strain relationship of soil based on the laboratory tests on creep [17]. In 1981, Mesri et al. used the hyperbolic function to simulate the one-dimensional stress-creep strain relationship of soil [18]. The Singh-Mitchell model cannot predict the creep deformation at low stress levels, while the Mesri model can accurately predict the entire strain-hardening process from zero strain to failure. Furthermore, the model parameters have clear physical significance. Hence, the Mesri model has been widely used. However, the Mesri model does not take into account the influence of the matric suction inside the unsaturated soil on the creep. In the present study, a modified one-dimensional Mesri creep model was established based on the proposed stress level.

The hyperbolic function of the Mesri model was used for the description:

$$\sigma_1 = \frac{\varepsilon}{\left(a' + b'\varepsilon\right)}. \tag{4}$$

In the formula, ε is the one-dimensional creep strain, and $1/a'$ is the initial tangent modulus of one-dimensional creep deformation, which is represented by E_d:

$$E_d = \left.\frac{d\sigma_1}{d\varepsilon}\right|_{\varepsilon=0} = \frac{1}{a'}. \tag{5}$$

$1/b'$ refers to the ultimate net vertical stress:

$$\sigma_{\text{ult}} = \lim_{\varepsilon\to\infty} \frac{\varepsilon}{a' + b'\varepsilon} = \frac{1}{b'}. \tag{6}$$

Since σ_{ult} can only be reached when the axial strain is infinite, while the failure stress used in practical engineering is usually reached under the finite strain ε_f, in order to make the one-dimensional stress-strain curve pass through the failure points $[\varepsilon_f, \sigma_f]$, the failure ratio was defined as $R_f = \sigma_f/\sigma_{\text{ult}}$, and the following can be obtained by substituting R_f and E_d into Formula (4):

Table 1: The initial physical property indexes of the undisturbed soil sample.

Soil sample depth/m	Natural density/(g/cm^3)	Natural moisture content/%	Liquid limit/%	Plastic limit/%	Plasticity index
2	1.68	17%	38.9	21.5	17.4

Table 2: Test scheme.

Matric suction s/kPa	Net vertical stress σ_1/kPa	Matric suction s/kPa	Net vertical stress σ_1/kPa	Matric suction s/kPa	Net vertical stress σ_1/kPa	Matric suction s/kPa	Net vertical stress σ_1/kPa
0	50	50	50	100	50	200	50
	100		100		100		100
	200		200		200		200
	300		300		300		300

$$\varepsilon = \frac{\sigma_f}{E_d} \cdot \frac{\sigma}{\sigma_f - R_f\sigma}. \tag{7}$$

The power function was selected to represent the one-dimensional creep-time relationship:

$$\varepsilon = \varepsilon_1 \left(\frac{t}{t_1}\right)^m. \tag{8}$$

In the formula, t is the time of creep deformation, t_1 is the reference time, which is usually taken as one minute, according to engineering experience, ε_1 is the strain when $t = t_1$, that is, the initial creep strain, and m is the slope of the curve $\lg\varepsilon - \lg t$.

By substituting Formula (8) into Formula (7), the Mesri creep equation can be obtained:

$$\varepsilon = \left[\frac{\sigma_f}{E_d}\right]_1 \cdot \frac{\sigma_1}{\sigma_f\text{-}(R_f)_1\sigma_1} \left(\frac{t}{t_1}\right)^m. \tag{9}$$

Formula (9) can also be written, as follows:

$$\frac{\varepsilon}{\sigma_1} = \left[\frac{\sigma_f}{E_d}\right]_1 \left(\frac{t}{t_1}\right)^m + \eta(R_f)_1\varepsilon. \tag{10}$$

It can be observed from Formula (1) that f is inversely proportional to σ_1. By substituting Formula (1) into Formula (10) and making a simplification, the following can be obtained:

$$f\varepsilon = \varsigma\left[\frac{\sigma_f}{E_d}\right]_1 \left(\frac{t}{t_1}\right)^m + \eta(R_f)_1\varepsilon. \tag{11}$$

In the formula, ς and η are the coefficients.

3.2. Test Verification. It can be observed from Formulae (8) and (11) that for different types of unsaturated soil, there are differences in parameter m. In order to verify the relationship between the unsaturated stress level and the creep strain of a specific kind of soil, the parameter m of the soil must be initially obtained. The present study carried out a one-dimensional creep laboratory test, in which the matric suction was controlled, and the net vertical stress was increased step by step for the viscous subsoil of an airport. The soil is taken from the viscous subgrade soil in Hefei area, and the study of such subgrade soil is of great theoretical significance for the engineering construction in eastern China.

The basic physical property indexes of the undisturbed soil sample are shown in Table 1. The undisturbed soil sample was made into 16 ring cutter samples, with a diameter of 61.8 mm and a height of 20 mm. The test instrument was the unsaturated soil consolidation instrument of Logistics Engineering College. Four kinds of matric suction were considered for the test: 0, 50, 100, and 200 kPa. The matric suction of 0 kPa was set for the contrast test of saturated soil. At the same time, four kinds of net vertical stresses were considered: 50, 100, 200, and 300 kPa. The specific test scheme is shown in Table 2.

Figure 1 shows the creep deformation amount-time correlation curve of the airport subsoil under different matric suctions. It can be observed that the laws of change in creep deformation amount over time under different conditions of matric suction are similar, which can be roughly divided into two stages: ① 0-1,500 minutes is the rapid deformation stage where the creep deformation amount rapidly grows as time increases; ② 1,500-15,000 minutes is the stable deformation stage where the creep deformation amount becomes gradually stable as time increases. Under the same conditions of net vertical stress, the creep deformation amount decreases as the matric suction grows, and the maximum creep deformation amount occurs at 0 kPa (saturated soil). This phenomenon again indicates that the matric suction has a certain hardening effect on the subsoil. Under the same conditions of matric suction, the creep deformation amount grows as the net vertical stress increases.

According to the deformation amount, the one-dimensional creep strain ε of each sample can be obtained, and the double logarithmic relation curve of the one-dimensional creep strain ε and the time t can be obtained. The curve $\lg\varepsilon - \lg t$ when $\sigma_1 = 50$ kPa is shown in Figure 2. It can be observed from the figure that the curve $\lg\varepsilon - \lg t$ shows a good linear relationship under different conditions of matric suction. This indicates that the time function of the one-dimensional creep strain of the unsaturated airport subsoil in the present study can be expressed with the power

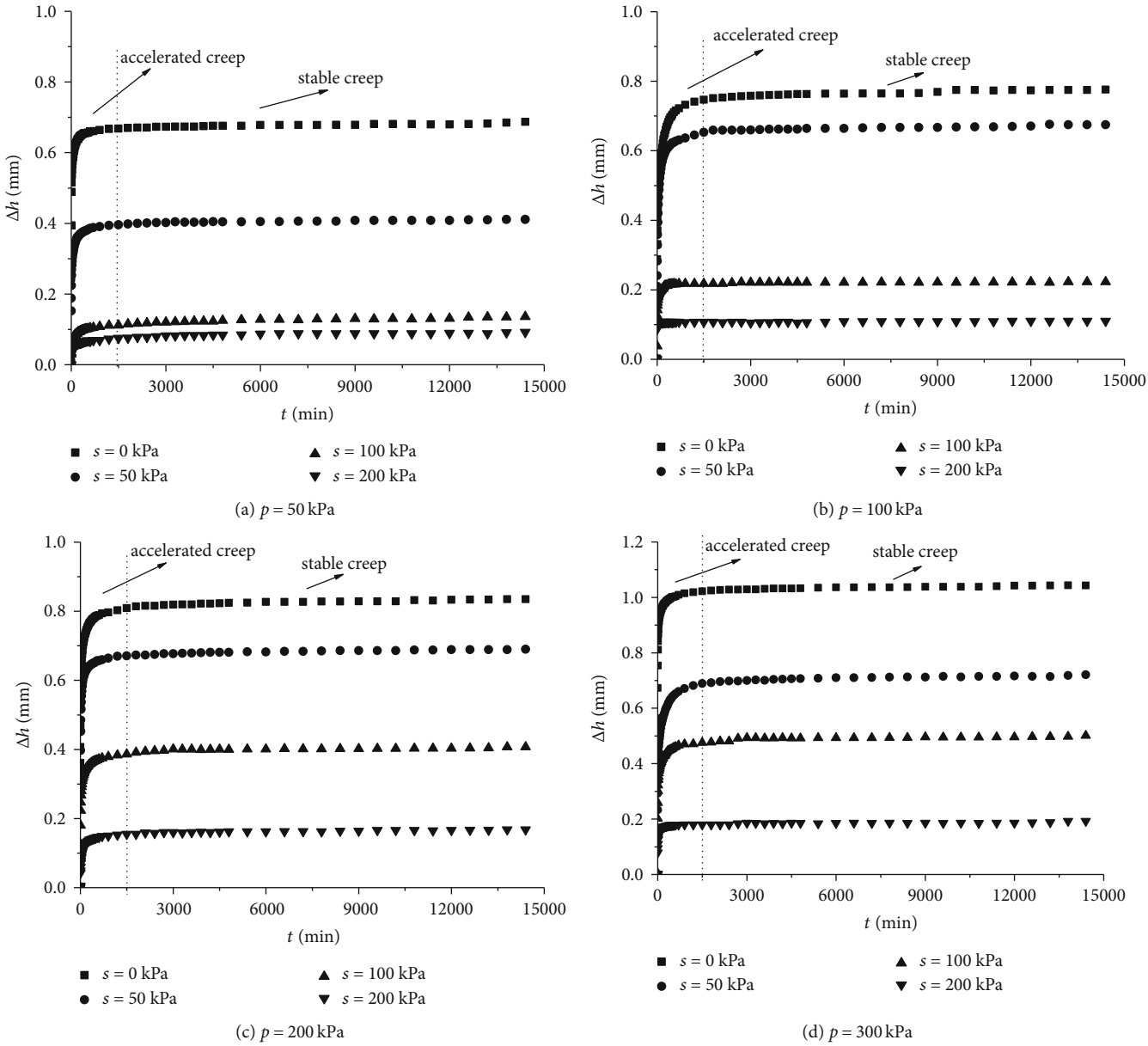

Figure 1: The deformation amount curve for the unsaturated soil samples with different matric suctions over time.

function. The relationship between the soil m and the matric suction s in the present study is as follows:

$$m = \partial_1 \cdot s^{\partial_2}. \tag{12}$$

In the formula, ∂_1 and ∂_2 are the corresponding fitting parameters.

Figure 3 presents the relation curve between m and the matric suction s when $\sigma_1 = 50$ kPa. It can be observed that Formula (12) can accurately express the relation of the soil in the present study.

By substituting Formula (12) into Formula (11), the one-dimensional Mesri creep model can be obtained, taking into account the matric suction for the unsaturated airport viscous subsoil in the present study:

$$f\varepsilon = \varsigma \left[\frac{\sigma_f}{E_d}\right]_1 \left(\frac{t}{t_1}\right)^{\partial_1 \cdot s^{\partial_2}} + \eta\left(R_f\right)_1 \varepsilon. \tag{13}$$

By applying Formula (12) to the one-dimensional creep-time characteristics when $p = 100$ kPa, as shown in Figure 4, it can be observed that the model fits well with the test values. This indicates that Formula (12) can be applied for the analysis of the creep characteristics of the unsaturated subsoil in the test section.

4. Three-Dimensional Creep Characteristics

In order to analyze the three-dimensional creep characteristics of the airport subsoil at different stress levels, the stress level-three-dimensional creep-time characteristics were first

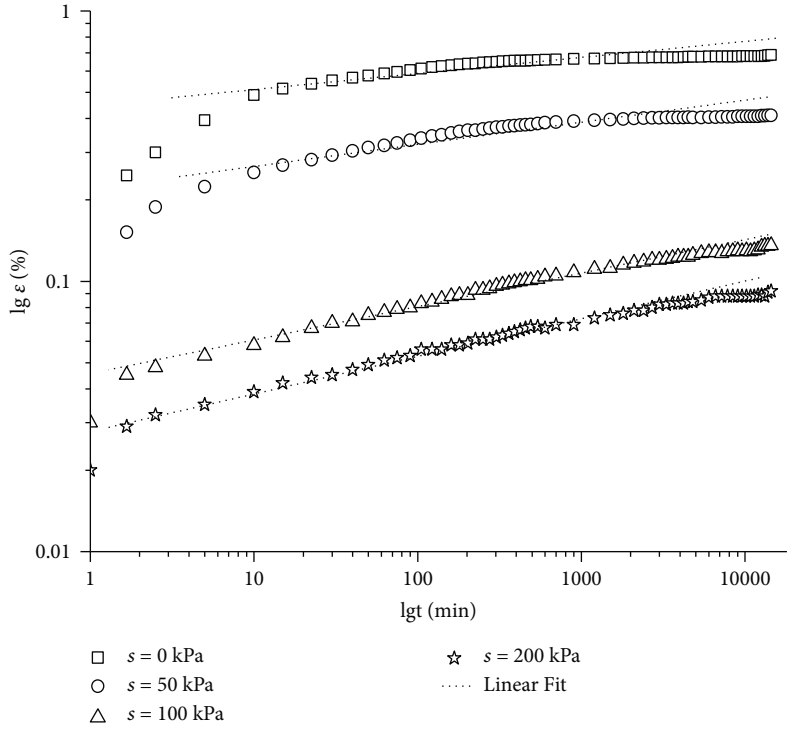

Figure 2: The curve lg ε – lg t of different matric suctions when $p = 50$ kPa.

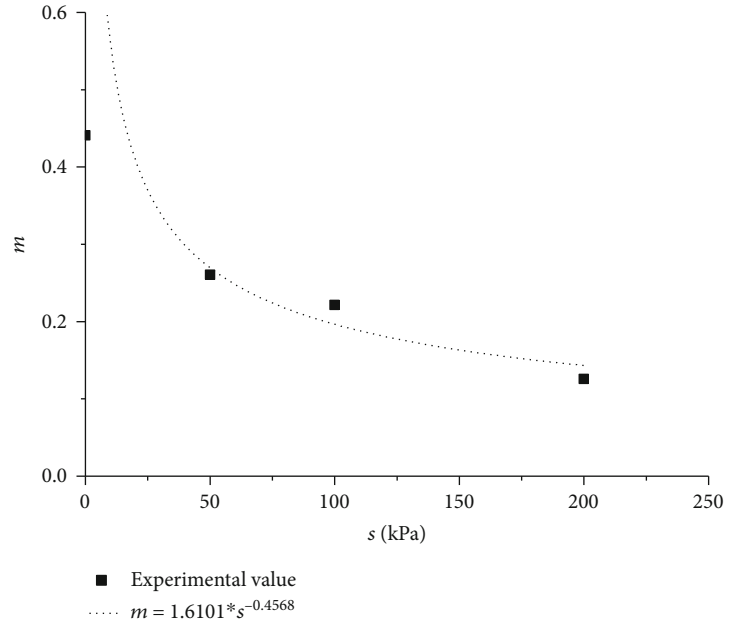

Figure 3: The relation curve of m and the matric suction s when $p = 50$ kPa.

analyzed based on laboratory tests. According to the test results, a three-dimensional creep model that took into account the unsaturated stress level was established for the test soil samples.

4.1. Stress Level-Three-Dimensional Creep-Time Characteristics. Triaxial creep tests were carried out under four stress levels. In such tests, the matric suction of soil was controlled by controlling the pore air pressure that was applied to the soil. In the test, the net mean stress was set at 200 kPa, and the matric suctions were set at 0, 50, 100, and 200 kPa. Hence, the stress levels for F were 0, 0.25, 0.5, and 1, respectively. The basic physical properties of the test soil samples were the same as those in the experiment in the previous section, as shown in Table 1. The undisturbed soil sample was made into four triaxial

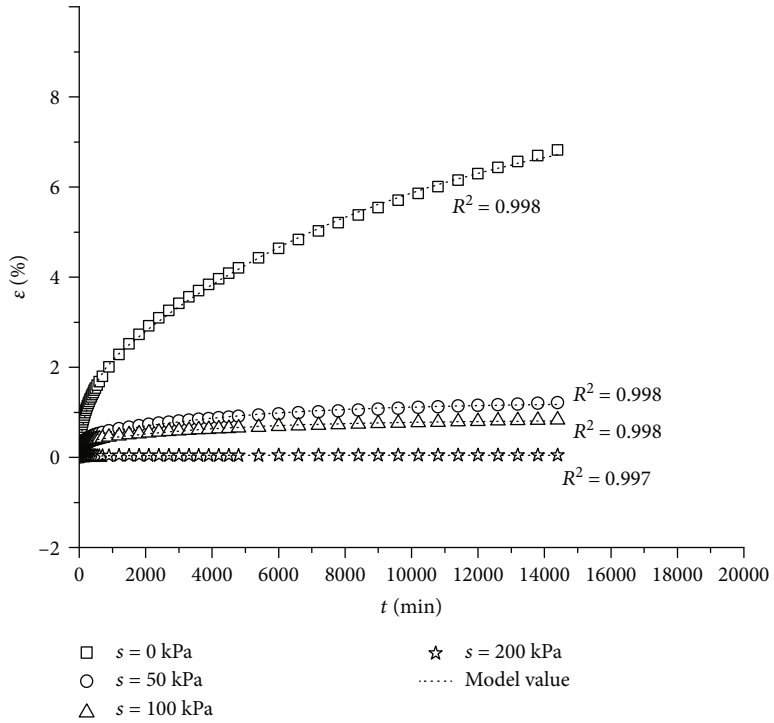

Figure 4: The curve $\varepsilon - t$ of different matric suctions when $p = 100$ kPa.

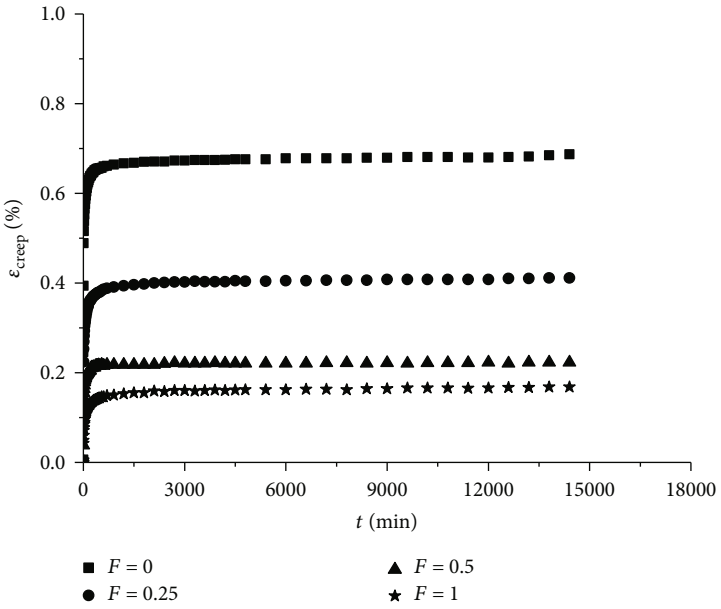

Figure 5: Time-varying curve of the creep strain of unsaturated soil samples under different stress levels.

samples, with a diameter of 39.1 mm and a height of 80 mm. At the same time, the four samples were tested with a net confining pressure of 100 kPa for the later model verification. According to the test results, the relationship between time and the three-dimensional creep strain of soil under different stress levels F can be obtained, as shown in Figure 5.

It can be observed from Figure 5 that the three-dimensional creep strain-time curve of unsaturated subsoil under different stress levels shows obvious nonlinear characteristics, and the strain-time relationship is similar to the hyperbolic function. Under isochronous conditions, the three-dimensional creep strain of the subsoil tends to decrease as F increases. The maximum creep strain of the subsoil occurs when $F = 0$ (at this point, $s = 0$ kPa, that is, the saturation state). The semilogarithmic coordinate of the time-varying creep strain shows a good linear variation relationship, as shown in Figure 6.

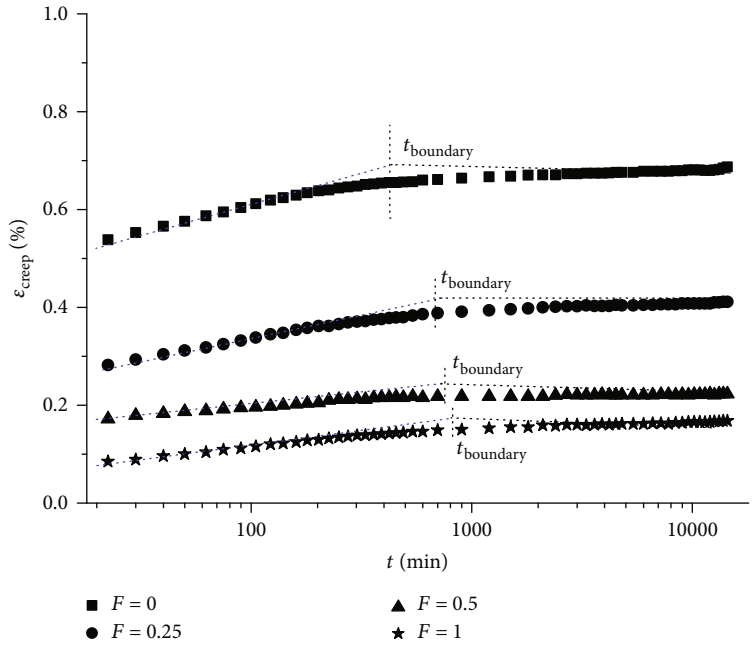

Figure 6: $\varepsilon - \lg t$ curve under different F.

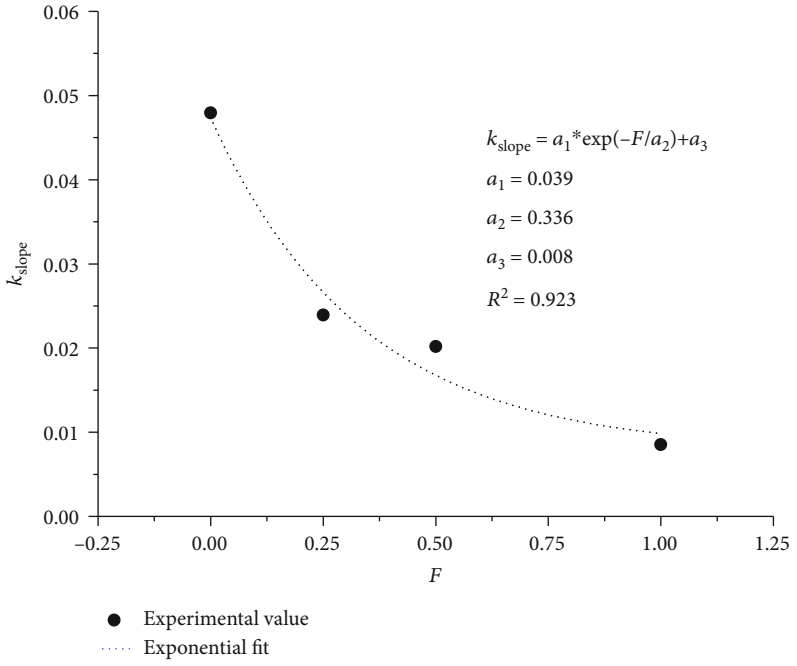

Figure 7: $k_{slope} \sim F$ relation curve.

It can be observed from Figure 6 that the curves $\varepsilon - \lg t$ under different F values were basically composed of two straight lines that represent the different creep deformation stages of the soil:

(1) The first straight line represents the accelerated creep stage, and the rate of change tends to slightly decrease as the value of F increases. The relationship between the rate of change and the value of F is shown in Figure 7. It can be observed from Figure 7 that there is a good exponential function relationship between the rate of change k_{slope} and the value of F:

$$k_{slope} = a_1 \cdot \exp\left(-\frac{F}{a_2}\right) + a_3. \quad (14)$$

In the formula, a_1, a_2, and a_3 are the fitting parameters.

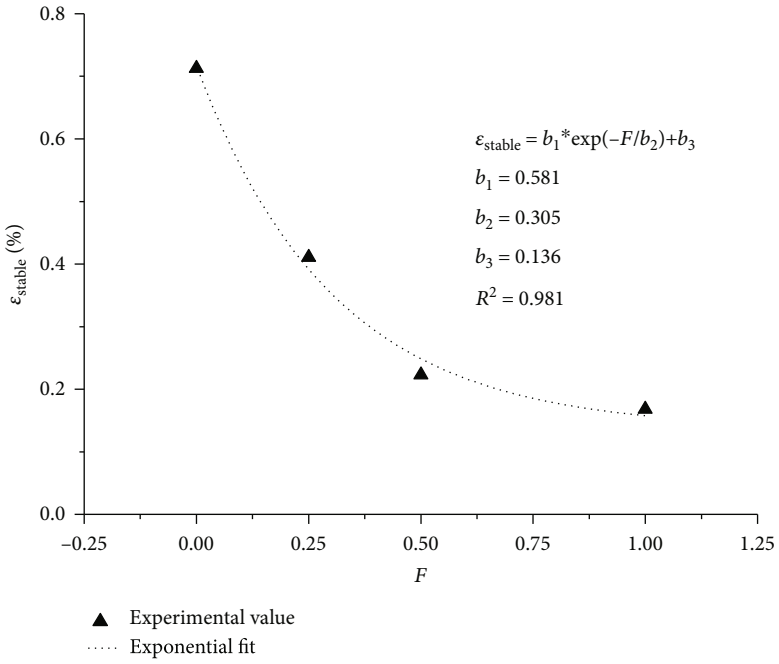

Figure 8: $\varepsilon_{stable} \sim F$ relation curve.

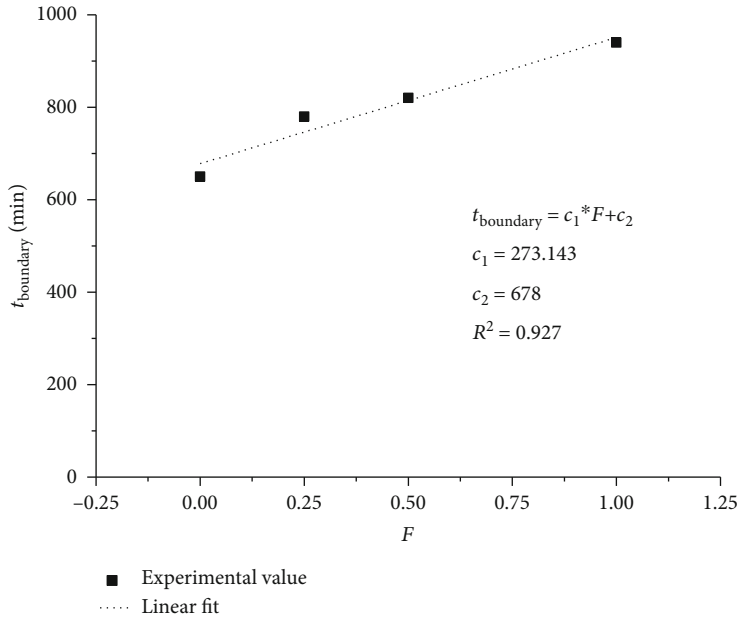

Figure 9: $t_{boundary} \sim F$ relation curve.

(2) The second straight line represents the stable creep stage. Under the condition of different F values, the creep deformation starts to reach stability. As the F value grows, the stability value ε_{stable} decreases. When the saturation state is reached (that is, $F = 0$), the maximum stability value occurs. The relationship between the stability value and F is shown in Figure 8. There is also a good exponential function relationship between the stability value and F:

$$\varepsilon_{stable} = b_1 \cdot \exp\left(-\frac{F}{b_2}\right) + b_3. \quad (15)$$

In the formula, b_1, b_2, and b_3 are the fitting parameters.

It can be observed in Figure 6 that the inflection points (that is, the time nodes of creep deformation) of the two straight lines in the curve $\varepsilon - \lg t$ under different F values were slightly different. Figure 9 shows the relationship

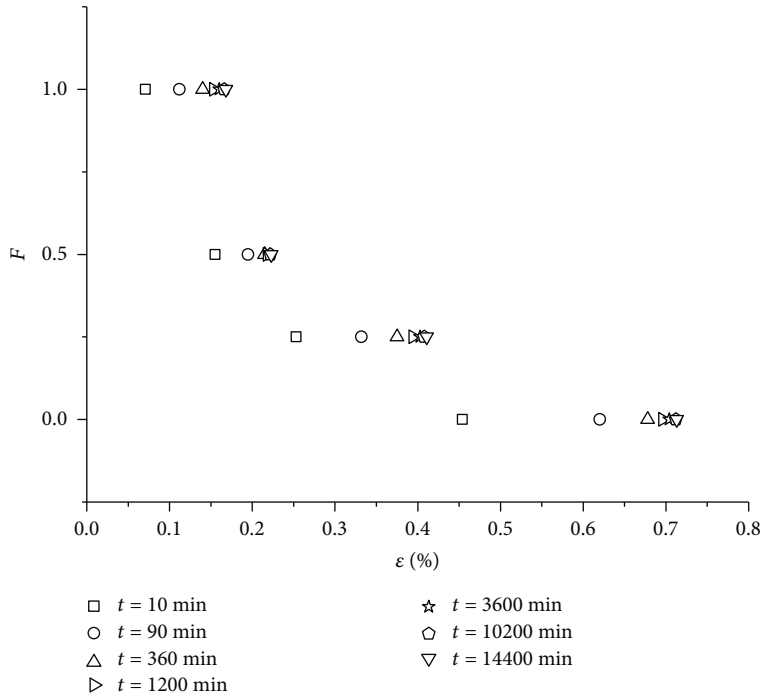

Figure 10: $F - \varepsilon$ curve (s=100 kPa).

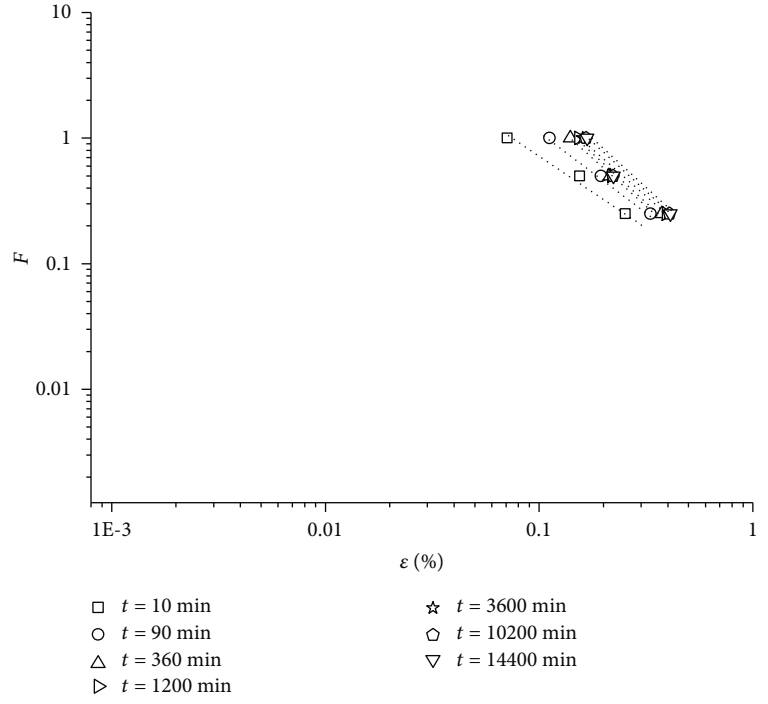

Figure 11: $F - \varepsilon$ curve (s=100 kPa).

between the time node of creep deformation and the value of F. It can be observed from Figure 5 that as the value of F increased, the time node of creep deformation t_{boundary} tended to increase. A roughly linear relationship exists between the time node of creep deformation and the value of F, and the relationship can be described by the following formula.

$$t_{\text{boundary}} = c_1 \cdot F + c_3. \tag{16}$$

In the formula, c_1 and c_2 are the fitting parameters.

In fact, the increase in matric suction inside the soil would strengthen the resistance of the soil to external forces. Under the same conditions, when the soil was subjected to

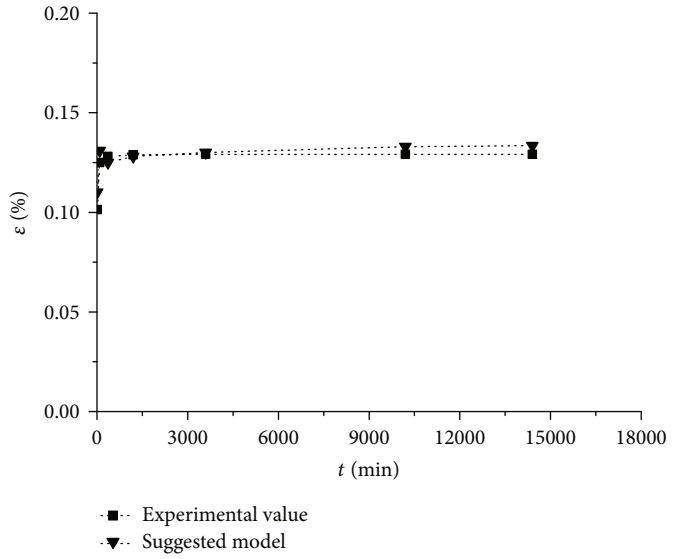

(a) $F = 0.25$ ($s = 25$ kPa)

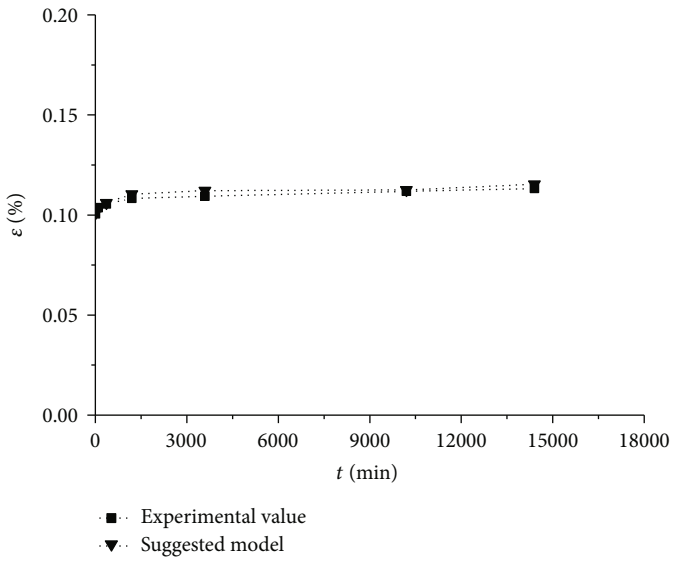

(b) $F = 0.5$ ($s = 50$ kPa)

Figure 12: Continued.

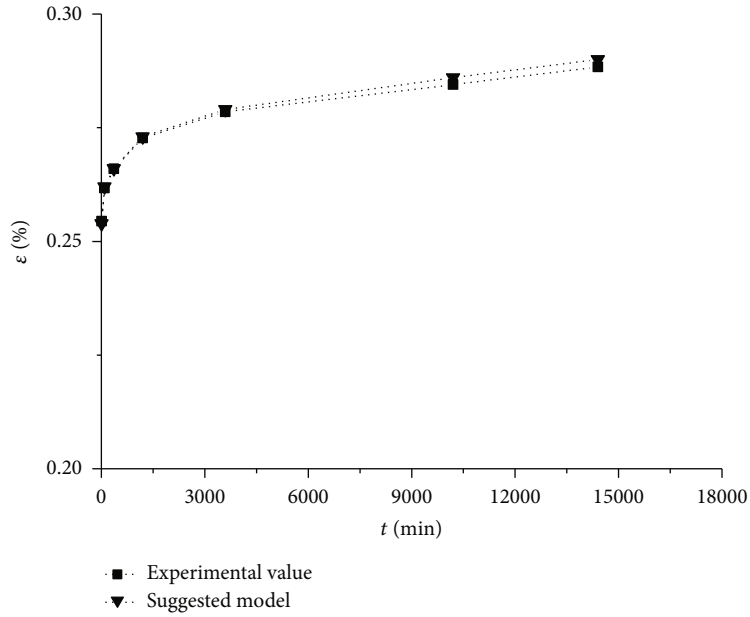

(c) $F = 1$ ($s = 100$ kPa)

Figure 12: Model validation (net mean pressure = 100 kPa).

constant stress, the deformation adjustment of the soil structure would become slower, and the time required for deformation stability would increase. Thus, as the value of F grows, t_{boundary} would increase. In practical railway foundation engineering, t_{boundary} represents the time when the subsoil can reach the final deformation stability, which has important engineering reference value for determining the railway track-laying time and operation time in the later stage.

4.2. The Three-Dimensional Creep Model with the Stress Level Taken into Account

4.2.1. Modeling. The test data was taken as an example for analysis when the net confining pressure was at 200 kPa. Figure 10 presents the stress-strain isochronal curve of the triaxial creep test of unsaturated viscous subsoil. It can be observed from the figure that the stress level-strain isochronous curve shows a good power function relationship. In combination with the test results in Figures 2, 10, and 11, the exponential function relationship was selected to describe the three-dimensional stress-creep strain relationship, and the hyperbolic function relationship was selected to describe the three-dimensional creep strain-time relationship, allowing a three-dimensional empirical creep model that takes into account the stress level to be established.

The expression of the three-dimensional creep model that takes into account the stress level is suggested, as follows:

$$\varepsilon = \Lambda_1 F^{\Lambda_3} \left(1 + \frac{t}{t_1}\right) / \left(1 + \Lambda_2 \frac{t}{t_1}\right). \tag{17}$$

In the formula, t is the duration of creep process (minutes), t_1 is the unit time (usually$t_1 = 1$ min), and Λ_1, Λ_2, and Λ_3 are the model parameters.

When $t = 0$, $\varepsilon_0 = \Lambda_1 F^{\Lambda_3}$. When $t = \infty$, $\varepsilon_\infty = \Lambda_1/\Lambda_2 F^{\Lambda_3} = \varepsilon_0/\Lambda_2$. In Formula (17), three parameters need to be determined, that is, Λ_1, Λ_2, and Λ_3. Since $\Lambda_2 = \varepsilon_0/\varepsilon_\infty$, the corresponding values of Λ_2 under different F can be calculated based on the test data. Through calculation, it is found that Λ_2 fluctuates around a fixed value. Hence, Λ_2 can be represented by its mean value, that is, Λ_2=0.2485. The relationship curve $\ln \varepsilon_0 \sim \ln F$ is drawn based on the test data, as shown in Figure 11. It can be observed from the figure that Λ_3 and $\ln \Lambda_1$ are the slope and intercept of the fitting straight line, respectively, and that $\Lambda_3 = 1.3809$ and $\ln \Lambda_1 = -1.5248$, that is, $\Lambda_1 = 0.2177$. Thus, the creep model established is as follows:

$$\varepsilon = 0.2177 F^{1.3809} \left(1 + \frac{t}{t_1}\right) / \left(1 + 0.2485 \frac{t}{t_1}\right). \tag{18}$$

4.2.2. Model Verification. Formula (18) was used to fit the test data with a net mean stress of 100 kPa. The fitting results are shown in Figure 12. It can be observed from the figure that the creep model value in the present is very close to the test value, which indicates that the creep model established in the present study can be used to analyze the law of strain-time change in the viscous subsoil of the test section under different stress levels.

5. Conclusions

In the present study, a new stress level of unsaturated soil was defined, and one-dimensional and three-dimensional laboratory tests and creep model studies were carried out for the actual airport viscous subsoil. The following conclusions are drawn:

(1) The ratio of the matric suction to the net vertical stress was proposed as the new unsaturated stress level f. Based on laboratory tests, it was found that the time function of one-dimensional creep strain shows a power function relationship and that the rate at which the creep strain changes over time exponentially decreases as the matric suction increases. Hence, the modified one-dimensional Mesri creep model is well applicable to the soil in the present study

(2) The ratio of the matric suction to the net mean stress was proposed as a new stress level. The power function was used to describe the relationship between three-dimensional stress and creep strain. Furthermore, the hyperbolic function was used to describe the relationship between three-dimensional creep strain and time. Hence, a three-dimensional creep analysis model that takes into account the stress level F for unsaturated soil was obtained

(3) The creep of unsaturated subsoil under different stress levels can be divided into the accelerated creep and stable creep. There was a good exponential function relationship between creep rate and F in both stages, and the time nodes of these two stages linearly decreased with the increase in F. The predicted value of the model established in the present can be well-matched with the test value. Thus, the model can be used to analyze the relationship between time and the creep strain of the viscous subsoil in the test section under different unsaturated stress levels

Data Availability

The figures presenting the test data analysis were all drawn in Origin 8.0. The data are available and explained in this article. Readers can access the data supporting the conclusions of this study. Also, all the data files used to support the findings of this study are available from the corresponding author upon request.

Conflicts of Interest

The authors declare that there are no conflicts of interest regarding the publication of this paper.

Authors' Contributions

Jun Feng and Yue Ma contributed to the conceptualization. Jun Feng, Yue Ma, and Zaobao Liu contributed to the methodology. Jun Feng and Zaobao Liu contributed to the validation. Jun Feng, Yue Ma, and Zaobao Liu contributed to the experiments. Jun Feng and Zaobao Liu contributed to the resources. Jun Feng and Yue Ma contributed to the data curation. Jun Feng and Yue Ma contributed to the writing—original draft preparation. Jun Feng and Zaobao Liu contributed to the writing—review and editing. Jun Feng and Zaobao Liu contributed to the project administration. Jun Feng, Yue Ma, and Zaobao Liu contributed to the project financial acquisition.

Acknowledgments

We gratefully acknowledge the School of airport engineering and transportation management, Civil Aviation Flight University of China, and the China Railway No.2 Engineering Group Co. LTD. for the financial support.

References

[1] Civil Aviation Administration of China, *MH/T5027-2013. Code for Design of Geotechnical Engineering for Civil Airports*, Civil Aviation Press of China, Beijing, 2013.

[2] E. Garcia, F. Oka, and S. Kimoto, "Numerical analysis of a one-dimensional infiltration problem in unsaturated soil by a seepage–deformation coupled method," *International Journal for Numerical and Analytical Methods in Geomechanics*, vol. 35, no. 5, pp. 544–568, 2011.

[3] Z. Han and S. K. Vanapalli, "Stiffness and shear strength of unsaturated soils in relation to soil-water characteristic curve," *Géotechnique*, vol. 66, no. 8, pp. 627–647, 2016.

[4] D. M. Pedroso, Y. Zhang, and W. Ehlers, "Solution of liquid–gas–solid coupled equations for porous media considering dynamics and hysteretic retention behavior," *Journal of Engineering Mechanics*, vol. 143, no. 6, article 04017021, 2017.

[5] X. N. Li, L. Wang, and J. Xu, "Study on the consolidation and settlement characteristics of unsaturated cohesive soil under pressure control," *Journal of Plateau Science*, vol. 3, no. 3, pp. 28–34, 2019.

[6] L. Z. Wu, J. Huang, W. Fan, and X. Li, "Hydro-mechanical coupling in unsaturated soils covering a non-deformable structure," *Computers and Geotechnics*, vol. 117, article 103287, 2020.

[7] H. J. Xiao, P. Hu, C. Y. Zeng, Y. Jia, and J. B. Wei, "Tests and sectional simulation of creep mechanical properties of unsaturated soils," *Science, Technology and Engineering*, vol. 20, no. 22, pp. 9133–9139, 2020.

[8] P. P. Sun, M. X. Zhang, T. F. Gu, M. M. Liu, X. Y. Dang, and Y. F. Zhao, "Creep characteristics of northern red clay under controlled suction," *Chinese Journal of Engineering Geology*, vol. 28, no. 3, pp. 500–509, 2020.

[9] S. Jeong, K. Lee, J. Kim, and Y. Kim, "Analysis of rainfall-induced landslide on unsaturated soil slopes," *Sustainability*, vol. 9, no. 7, p. 1280, 2017.

[10] M. A. Alfaro Soto, H. K. Chang, and M. T. van Genuchten, "Fractal-based models for the unsaturated soil hydraulic functions," *Geoderma*, vol. 306, no. 15, pp. 144–151, 2017.

[11] S. E. Cho, "Stability analysis of unsaturated soil slopes considering water-air flow caused by rainfall infiltration," *Engineering Geology*, vol. 211, no. 23, pp. 184–197, 2016.

[12] J. Kim, Y. Kim, S. Jeong, and M. Hong, "Rainfall-induced landslides by deficit field matric suction in unsaturated soil slopes," *Environmental Earth Sciences*, vol. 76, no. 23, pp. 1–17, 2017.

[13] Y. Chen, F. Marinelli, and G. Buscarnera, "Mathematical interpretation of delayed instability in viscous unsaturated soil," *Géotechnique Letters*, vol. 9, no. 3, pp. 165–172, 2019.

[14] N. Lu and C. Zhang, "Soil sorptive potential: concept, theory, and verification," *Journal of Geotechnical and Geoenvironmental Engineering*, vol. 145, no. 4, article 04019006, 2019.

[15] S. K. Ma, M. S. Huang, P. Hu, and C. Yang, "Soil-water characteristics and shear strength in constant water content triaxial tests on Yunnan red clay," *Journal of Central South University*, vol. 20, no. 5, pp. 1412–1419, 2013.

[16] W. Fuentes and T. Triantafyllidis, "Hydro-mechanical hypoplastic models for unsaturated soils under isotropic stress conditions," *Computers and Geotechnics*, vol. 51, pp. 72–82, 2013.

[17] A. M. J. K. Singh, "General stress-strain-time function for soils," *Journal of Soil Mechanics and Found Engineering Division, ASCE*, vol. 94, no. 1, pp. 21–46, 1968.

[18] G. R. E. S. Mesri, E. Febres-Cordero, D. R. Shields, and A. Castro, "Shear stress-strain-time behaviour of clays," *Géotechnique*, vol. 31, no. 4, pp. 537–552, 1981.